

Platelet-rich Plasma Promotes Healing of Osteoporotic Fractures

LINWEI CHEN, MD; XIAOBO YANG, MD; GAO HUANG, MS; DIANWEN SONG, MD; XUE-SHI YE, MD; HUAZI XU, BS; WANLI LI, MD

With an aging population worldwide, the frequency of osteoporotic fractures is increasing. Therefore, biological methods to enhance the internal fixation of osteoporotic fractures becomes more important to reduce the societal burden of care. The purposes of this study were to evaluate the role of platelet-rich plasma (PRP) in the treatment of osteoporotic fractures and to clarify the best concentration of PRP. Bone marrow mesenchymal stem cells isolated from osteoporotic rats were cultured in high- ($8.21 \pm 0.4 \times 10^9/\text{mL}$), medium- ($2.65 \pm 0.2 \times 10^9/\text{mL}$), and low-concentration ($0.85 \pm 0.16 \times 10^9/\text{mL}$) PRP and in platelet-poor plasma ($8 \pm 0.5 \times 10^6$ platelet/mL). The capacities of cell proliferation and osteogenic and adipogenic differentiation were compared. A transverse osteotomy was performed in the middle of the left femoral diaphysis followed by K-wire fixation, and various concentrations of PRP were transplanted into the fracture zone. Radiologic, mechanical, and histologic evaluations were performed at 2, 4, and 8 weeks, respectively. The results indicated that PRP could inhibit adipogenic differentiation and that medium-concentration PRP was effective in inducing the proliferation and osteogenic differentiation of bone marrow mesenchymal stem cells derived from osteoporotic bone marrow and in promoting fracture healing, whereas high-concentration PRP inhibited osteogenic differentiation and callus remodeling. Certain concentrations of PRP can effectively enhance the healing of osteoporotic fractures. Medium-concentration PRP is a suitable concentration to use in practice.

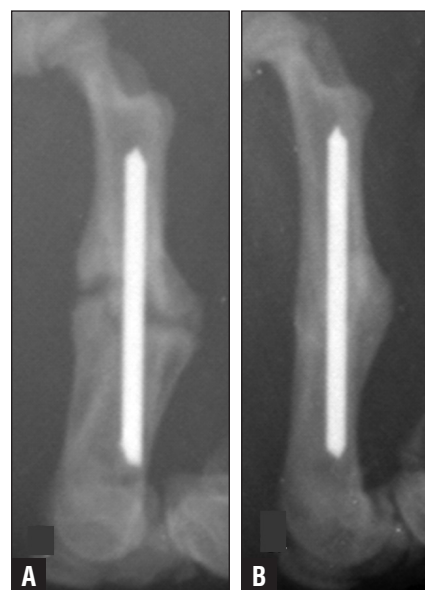


Figure: Radiographs taken 8 weeks after injections. The control group showed evident callus but a fracture gap that did not bridge (A). The medium-concentration alkaline phosphatase group showed perfect fracture union (B).

The authors are from the Department of Orthopedics (LC, XY, WL), Second Affiliated Hospital, School of Medicine; the Department of Hematology (X-SY), Sir Run Run Shaw Hospital, School of Medicine, Zhejiang University, Hangzhou; the Department of Orthopedics (GH, HX), Second Affiliated Hospital of Wenzhou Medical College; the Department of Orthopedics (LC), Second Affiliated Hospital of Wenzhou Medical College, Wenzhou, Zhejiang Province; and the Department of Orthopedics (DS), Chang Zheng Hospital, Second Military Medical University; Shanghai, China.

The authors have no relevant financial relationships to disclose.

Supported by the Wenzhou Science & Technology Foundation (2010S0555); National Natural Science Foundation of China (NSFC) (30901511); Natural Science Foundation of Zhejiang Province (Y2090065). The fund belongs to the Wenzhou Science & Technology Foundation (2010S0555); the National Natural Science Foundation of China (NSFC) (30901511); and the Natural Science Foundation of Zhejiang Province (Y2090065).

Correspondence should be addressed to: Wanli Li, MD, Department of Orthopedics, Second Affiliated Hospital, School of Medicine, Zhejiang University, Hangzhou, 310009, China (surgeonlinwei@163.com).

doi: 10.3928/01477447-20130523-10

Osteoporosis has become one of the most prevalent diseases for the elderly in the developed and some developing countries. It is characterized by a systemic impairment of bone mass and microarchitecture that results in fragility fractures.¹ Fracture healing in osteoporotic bone is characterized by reduced callus formation, impaired biomechanical properties of newly formed bone, and a prolonged fracture healing process.² Bone resorption proceeds more rapidly than bone formation. Recent data suggested that bone marrow mesenchymal stem cells (BMSCs) isolated from osteoporotic bones exhibit a lower proliferation rate and adipogenic differentiation, leading to the accumulation of adipose tissue in bone.³ The increased adipogenesis and decreased osteogenesis of BMSCs are correlated with the impaired process of fracture healing. It is recommended that some greater osteogenic stimuli are requisite in accelerating the osteoblastogenesis of BMSCs derived from osteoporotic

bone marrow, thus promoting the healing of osteoporotic fractures.

Growth factors offer the potential to shorten the time and improve the quality of fracture repair.⁴ Various growth factors, such as bone morphogenic protein-2 and platelet-derived growth factors, have been used to enhance the repair of osteoporotic fractures.^{4,5} Platelet-rich plasma (PRP) contains multiple growth factors, such as platelet-derived growth factors and transforming growth factor- β (TGF- β), that accelerate BMSC proliferation and enhance BMSC osteogenic differentiation.⁶ Meanwhile, PRP has been used successfully in the acceleration of bone fracture healing, such as common fracture healing, diabetic fracture healing, and nonunion.⁶⁻⁹ However, the applications of PRP in osteoporotic fracture healing and its suitable concentration have not been reported.

The aim of this study was to examine the effect of administering different concentrations of PRP on the proliferation and differentiation of MSCs derived

from osteoporotic bone and on the healing of osteoporotic fracture in vivo. The authors hypothesized that PRP could induce the proliferation and osteogenic differentiation of BMSCs and promote the bone healing of osteoporotic fractures. To the authors' knowledge, this is the first study that describes the relationship

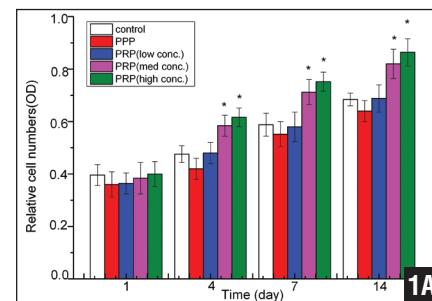


Figure 1: Graph showing the proliferation of bone marrow mesenchymal stem cells at days 1, 4, 7, and 14. Bone marrow mesenchymal stem cells cultured in high- and medium-concentration platelet-rich plasma showed a significant increase in the proliferation of bone marrow mesenchymal stem cells compared with the other groups on days 1, 4, 7, and 14 ($P < .05$). * $P < .05$.

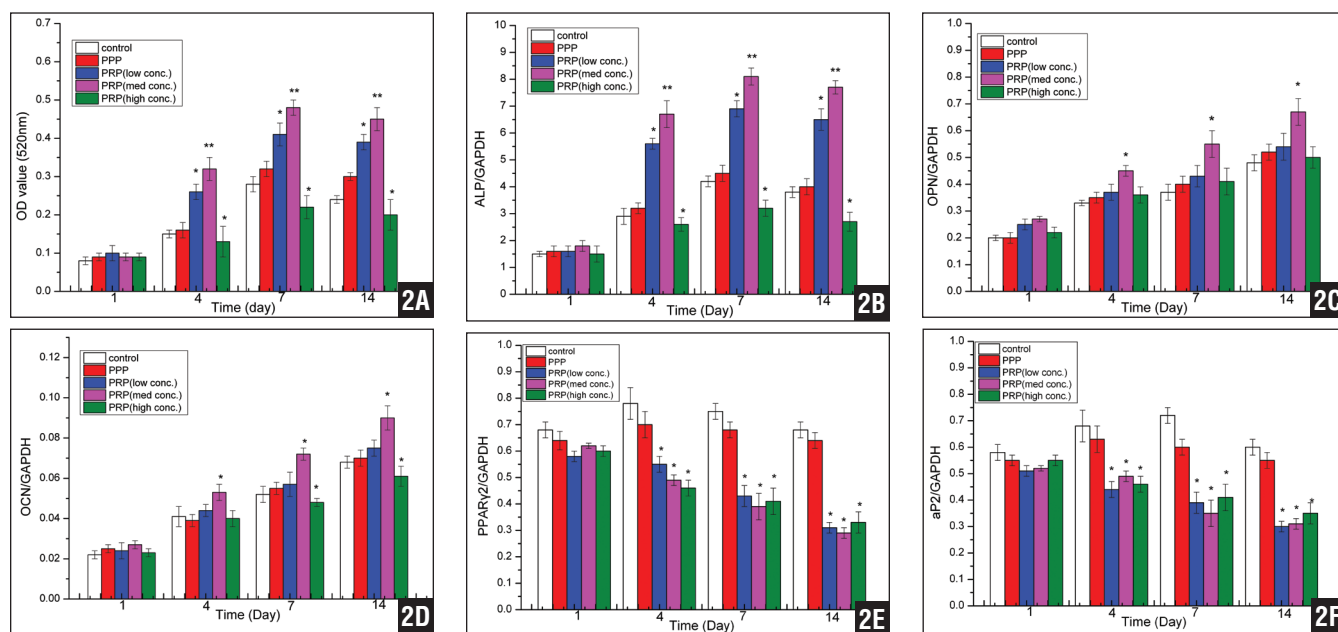


Figure 2: The alkaline phosphatase activity was significantly increased in low- and medium-concentration platelet-rich plasma (PRP) ($P < .01$) and was inhibited in high-concentration PRP (A). The expression of alkaline phosphatase messenger ribonucleic acid was significantly increased in low- and medium-concentration PRP and decreased in high-concentration PRP (B). Osteopontin messenger ribonucleic acid expression level was up-regulated in medium-concentration PRP (C). Osteocalcin expression was up-regulated in medium-concentration PRP and down-regulated in high-concentration PRP (D). Peroxisome proliferator-activated receptor messenger ribonucleic acid expression level was down-regulated in PRP-contained groups (E). The adipocyte protein 2 expression decreased in PRP-contained groups (F). * $P < .05$, ** $P < .01$.

between PRP and osteoporotic fracture healing.

MATERIALS AND METHODS

The study was approved by the University of Animal Care and Use Committee of Wenzhou Medical College.

Animals

Sprague-Dawley rats (Wenzhou, Zhejiang, China) weighing between 200 to 250 g were ovariectomized when the rats were aged 6 months and were then housed for 6 months to induce osteoporosis. Bone mineral density was measured using dual-energy X-ray absorptiometry scanning.¹⁰ Bone mineral density decrease was detected at the fifth lumbar vertebra, the right femoral shaft, and right femoral head shaft in 8.7% ($P=.01$), 7.6% ($P=.037$), and 9.6% ($P=.023$) of rats, respectively, compared with those before ovariectomy.

Platelet-rich Plasma Preparation

Whole blood was extracted via open chest cardiac puncture in ovariectomized rats. Platelet-rich plasma was prepared using a 2-step centrifugation process.¹¹ Briefly, whole blood was initially centrifuged at 220 g for 15 minutes to separate the plasma portions from the red blood cell fraction. The plasma portions were centrifuged again at 980 g for 10 minutes to separate the PRP from the platelet-poor plasma (PPP). The PRP was divided into 3 concentrations according to the amount of PPP that was removed. The platelet concentrations in whole blood, PPP, and PRP were determined automatically by a hematology analyzer (Sysmex KX-21; Sysmex, Tokyo, Japan). Then, the PRP (3 concentrations) and PPP were mixed with a thrombin/ CaCl_2 solution to obtain a fibrin clot ($v/v=10:1$). The fibrin clot was centrifuged at 5000 rpm for 15 minutes, and the supernatant platelet-rich clot releasate (PRCR) and platelet-poor clot releasate (PPCR) were carefully transferred to sterile centrifuge tubes. The platelet-derived growth factor-AB and transform-

Table 1

Real-time PCR Primer Sequences for Osteoblastic Differentiation Markers

Target Gene	Sequence (5'→3')
OCN	Forward GAG GAC CCT CTC TCT GCT CAC TCT GCT GG
	Reverse CCT CTC TCT GCC TCG AAA GTA TGG AC
OPN	Forward ATG AGA TTG GCA GTG ATT
	Reverse GTT GAC CTC AGA AGA TGA
ALP	Forward CGG ACC CTG CCT TAC CAA CTC ATT TGT GCC
	Reverse CGC ACG CGA TGC AAC ACC ACT CAG G
PPAR γ 2	Forward CTCTGGGAGATTCTCTGTTGA
	Reverse GGTGGGCCAGAATGGCATCT
aP2	Forward TCTCCAGTGAA AACTTCGAT
	Reverse TTACGCTGATGATCATGTTG
GAPDH	Forward GCT CTC CAG AAC ATC ATC CCT GCC
	Reverse CGT TGT CAT ACC AGG AAA TGA GCT T

Abbreviations: ALP, alkaline phosphatase; aP2, adiponectin, adipisin; GAPDH, glyceraldehyde-3-phosphate-dehydrogenase; OCN, osteocalcin; OPN, osteopontin; PCR, platelet clot releasate; PPAR γ 2; peroxisome proliferator-activated receptor.

Table 2

Radiographic Scoring System for Fracture Healing^a

Categories	Scores			
	3	2	1	0
Callus formation	Full across the defect	Moderate (>50%)	Mild (<50%)	None
Bone union	Full bone bridge	Moderate (>50%)	Mild (<50%)	None
Cortex remodeling		Full	Mild (<50%)	None

^aMaximum expected score is 8 for bone fracture repair. Bone union was defined as complete mineralized callus bridging of all 4 cortices on both anteroposterior and lateral radiographs.

Table 3

Three-point Load Bearing^a

Biomechanical Index	Control	PPP	PRP Concentration		
			Low	Medium	High
Ultimate load (N)	60.2±1.0	62.2±1.6	69.4±2.3	92.3±3.1 ^b	68.6±2.3
Stiffness (N/mm)	21.4±9.8	23.5±4.7	29.6±4.8	36.5±7.1 ^b	28.8±5.4

Abbreviations: PPP, platelet-poor plasma; PRP, platelet-rich plasma.

^aLoad to failure value and stiffness were higher in PRP-containing groups than the control and PPP groups.

^bSignificant differences were only detected in medium-concentration PRP. $P<.05$.

ing growth factor (TGF- β 1) levels in the supernatant were measured using a commercially available ELISA kit (Pepro-Tech, Rocky Hill, New Jersey) as previously described.¹¹

Isolation and Culture of Bone Marrow Mesenchymal Stem Cells

During exsanguination, the femoral bone was harvested intraoperatively and washed with growth culture medium (Gibco, Carlsbad, California) supplemented with 10% (v/v) fetal bovine serum (Gibco). The cell suspensions were plated and incubated in a humidified atmosphere of 5% CO₂ at 37°C. PRCR and PPCR were added to serum-free standard culture medium (Gibco) supplemented with 1% (v/v) penicillin and streptomycin (Gibco) to the concentration of 10%. Bone marrow mesenchymal stem cells were seeded in the 10% PRCR medium, 10% PPCR medium, and 10% fetal bovine serum containing a standard culture medium as a control.

Bone Marrow Mesenchymal Stem Cells Proliferation

Bone marrow mesenchymal stem cells were cultured in 96-well plates at 2×10⁴ cells per well with different growth culture mediums. After culturing for 1, 4, 7, and 14 days, the cell counting kit-8 assay was performed according to the cell proliferation kit protocol (Sigma, Shanghai, China). Then, the optical density was read

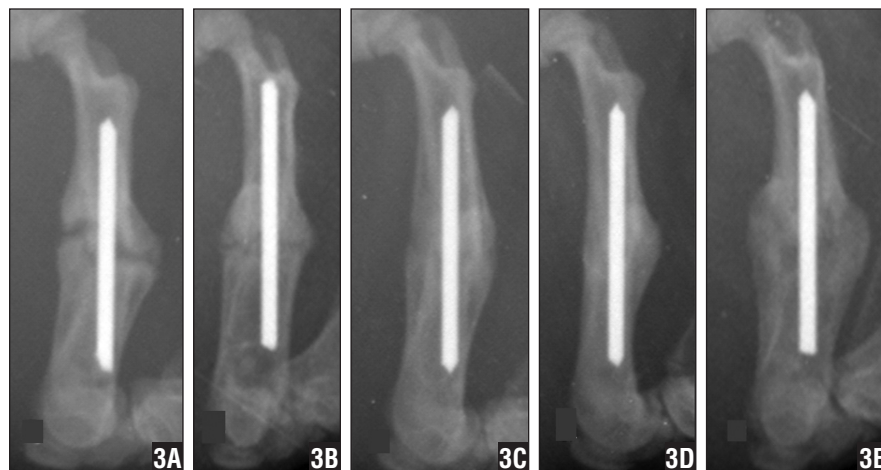


Figure 3: Radiographs taken 8 weeks after injections. The control group showed evident callus but the fracture gap did not bridge (A). The platelet-poor plasma group showed callus formation with bridging of the fracture gap with only faint fracture line (B). The low-concentration platelet-rich plasma group showed callus formation with bridging of the fracture gap with only a faint fracture line (C). The medium-concentration alkaline phosphatase group showed perfect fracture union (D). The high-concentration platelet-rich plasma group showed fracture union with a faint fracture line and a large callus (E).

on microplate reader (Bio-RadModel 550; Bio-Rad, Hercules, California) at 450 nm.¹² This test was repeated 3 times.

Alkaline Phosphatase Activity Assay

At 1, 7, and 14 days of culture, the alkaline phosphatase (ALP) activity level was determined. Briefly, cells were rinsed with phosphate-buffered saline followed by trypsinization and scraped into double-distilled H₂O. The ALP activity was measured using p-nitrophenyl phosphate (Sigma) as the substrate at 405 nm, and the total protein contents were measured with the bicinchoninic acid method.¹¹ The ALP activity level was normal-

ized to the total protein content. This test was repeated 3 times.

Real-time Polymerase Chain Reaction for Osteogenic and Adipogenic Differentiation Marker

Real-time PCR was used to detect the expression of several osteogenic differentiation-related marker genes (eg, ALP, osteocalcin, osteopontin) and 2 adipogenic differentiation-related marker genes [peroxisome proliferator-activated receptor; aP2 (adiponectin, adipisin)] at 1, 4, 7, and 14 days. Total ribonucleic acid was extracted using TriZol (Invitrogen, Carlsbad, California) and quantified spectrophotometrically at

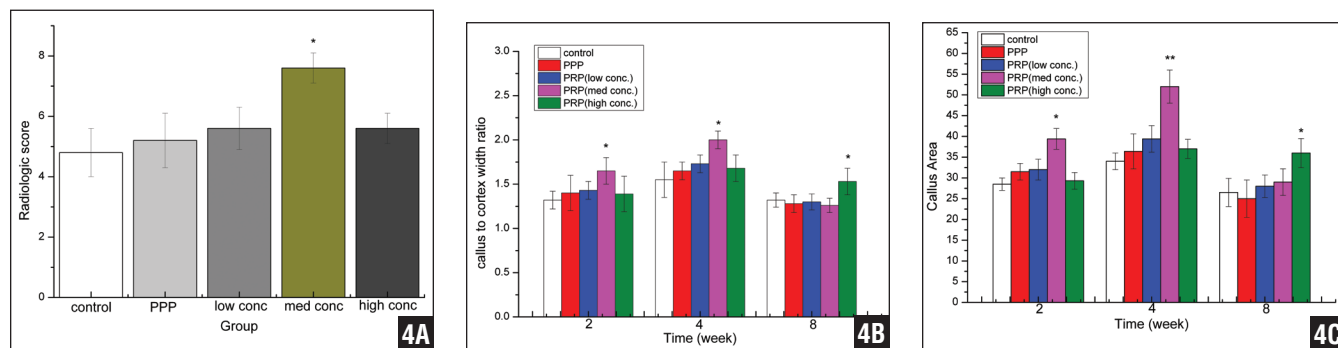


Figure 4: Graphs. Radiological scoring of the radiographs on late phase of fracture healing (A). Quantitative analyses of callus to cortex width ratio (CW) (maximal callus width divided by the outer diameter of the femur) (B) and callus area (CA) (the areas of the external mineralized callus) (C). *P<.05, **P<.01.

260 nm (HP 8452A diode array spectrophotometer). First-strand complementary DNAs (cDNAs) were reverse-transcribed from total ribonucleic acid of each sample by oligo-(dT) primer using the DyNamo™ cDNA synthesis kit (Fermentas, Burlington, Canada). Real-time PCR using the iCycler PCR system (Bio-Rad, Munich, Germany) was performed with the single-stranded cDNA sample (SYBR Green Master mix; Tiangen, Beijing, China). Relative expression levels of each target gene were normalized by the value of the housekeeping GAPDH gene. Primer's sequences of the targeted genes are shown in Table 1. This test was repeated 3 times.

Surgical Technique

Following anesthesia, a transverse osteotomy was performed in the middle of the left femoral diaphysis with a saw. Internal fixation of the fracture was achieved

by inserting a 1.2-mm K-wire retrograde into the intramedullary canal. For the experimental groups, a 500- μ l activated platelet-rich clot (best concentration for BMSCs) was placed circumferentially around the osteotomy and the soft tissues were closed. For the control group, the same amount of saline was placed around the osteotomy.

Radiographic Evaluation

Each group underwent radiologic evaluation at 2, 4, and 8 weeks after injection. Radiographs of the left femurs were taken using a Philips Digital Diagnost/Optimus 80 system (Philips, Eindhoven, Netherlands) at 46 kV, 2.5 mAs, and 10.6 ms of exposure. Fracture healing was staged on the radiographs using a radiographic modified scoring system (Table 2).⁴ Callus to cortex width ratio (maximal callus width divided by the outer diameter of the femur) was recorded. Callus

area was measured as the sum of the areas of the external mineralized callus by Metamorph Image Analysis System. All radiographs were randomized and independently assessed by a qualified radiologist who was unaware of which treatment the rats had received (G.H.).

Three-point Load Bearing

After removing the intramedullary pin at week 8, femurs (n=6 per group) were placed on 2 rounded bars in a biomechanical machine (Model LS 500; Lloyd, Southampton, United Kingdom) at a distance of 32 mm at a constant displacement rate of 5 mm per minute. Force was applied at the fracture line from above until refracture occurred. The ultimate load and stiffness were recorded and analyzed.

Histologic Evaluation

At 2, 4, and 8 week after injection, 6 bone specimens per group were fixed in 10% formalin for 1 week followed by decalcification in formic acid. Specimens were cut into 15- μ m cryostatic sections and fixed in 2% paraformaldehyde. Hematoxylin-eosin staining was performed as follows: cryostatic sections were stained for 15 seconds in Harris hematoxylin and 15 seconds in eosin solution, washed in H₂O, and dehydrated in successive ethanol. Stained sections were observed with a Leica DMR microscope (Leica Microsystems, Buffalo, New York); images were acquired using the Leica DC500 digital camera (Leica). All stained sections were randomized and independently assessed by a histologist who was unaware of which treatment the rats had received (X.Y.).

Statistical Analysis

All quantitative data were expressed as mean \pm SD and analyzed with SPSS version 17.0 software (SPSS, Inc, Chicago, Illinois). Analysis of variance was verified using the Bartlett test. Differences in data among each group were compared using the Student-Newman-Kuels-q test. Statis-

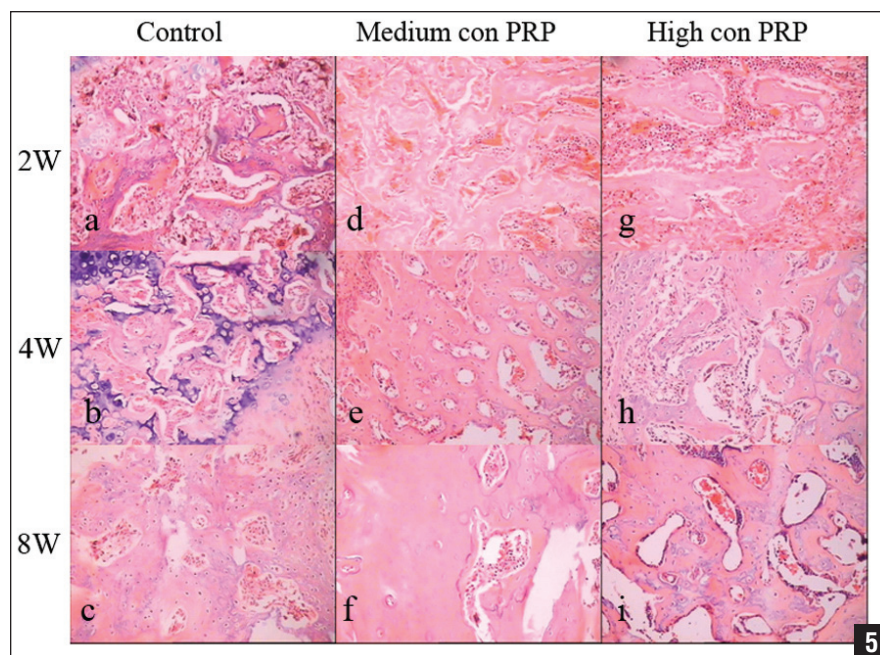


Figure 5: Representative histological sections of the medium- and high-concentration platelet-rich plasma (PRP) groups and control group at different time points, stained with hematoxylin-eosin (original magnification, $\times 100$). Two weeks after treatment, newly formed woven bone, inflammatory cells, and vessels were observed (a, d, g). At week 4, the control group mainly demonstrated woven bone and cartilage islands (b). The medium-concentration PRP showed more than 50% trabecular bone formation and cortex remodeling (e). The high-concentration PRP group showed less than 50% trabecular bone formation (h). At week 8, the control group showed immature bone trabeculae and chondroid tissue (c). The medium-concentration PRP group showed mature trabecular bone and cortex remodeling (f). The high-concentration PRP group showed loosely and irregularly arranged trabecular bone (i).

tical significance was set at a P value less than .05.

RESULTS

Properties of Platelet-rich and -poor Plasma

The platelet count (platelets per mL) was $8.21 \pm 0.4 \times 10^9/\text{mL}$ in high-concentration PRP, $2.65 \pm 0.2 \times 10^9/\text{mL}$ in medium-concentration PRP, $0.85 \pm 0.16 \times 10^9/\text{mL}$ in low-concentration PRP, $8 \pm 0.5 \times 10^6/\text{mL}$ in PPP, and $0.67 \pm 0.04 \times 10^9/\text{mL}$ in whole blood. The contents of TGF- β 1 in PRP were 56.4 ± 1.3 , 155.6 ± 2.4 , and 530.2 ± 15.4 ng/mL, respectively. The contents of platelet-derived growth factor-AB in PRP were 20.3 ± 1.2 , 56.9 ± 6.3 , and 185.5 ± 23.4 pg/mL, respectively.

Proliferation of BMSCs

Bone marrow mesenchymal stem cells cultured in high- and medium-concentration PRP showed a significant increase in the proliferation of BMSCs compared with the other groups on days 1, 4, 7, and 14 ($P < .05$). No significant differences were found among the other 3 groups ($P > .05$) (Figure 1).

Osteogenic and Adipogenic Differentiation of Bone Marrow Mesenchymal Stem Cells

On days 4, 7, and 14 after injection, the ALP activity was significantly increased in low- ($P < .05$) and medium-concentration PRP ($P < .01$) and was inhibited in high-concentration PRP ($P < .05$) (Figure 2A). Medium-concentration PRP showed the highest ALP activity compared with the other groups. Similarly, the expression of ALP messenger ribonucleic acid was significantly increased in low- ($P < .05$) and medium-concentration PRP ($P < .01$) and decreased in high-concentration PRP ($P < .05$) (Figure 2B). Osteopontin and osteocalcin messenger ribonucleic acid expression level was up-regulated in medium-concentration PRP ($P < .05$). Osteocalcin expression decreased in high-concentration PRP compared with the other groups ($P < .05$), whereas no significant

differences existed in the other groups (Figures 2C, D). Significantly lower peroxisome proliferator-activated receptor and α 2 were observed in all PRP-contained groups compared with the PPP and control groups ($P < .05$) (Figures 2E, F).

Radiographic Evaluation

The medium-concentration PRP group showed faster healing than the other groups, with a faster bridging of the fracture gaps and higher bridging rate (Figure 3). At week 8 after injection, the mean radiological score was higher in the medium-concentration PRP group than the other groups with callus formation ($P < .05$) (Figure 4A). All fractures achieved radiographic healing in the medium-concentration group compared with 10 (67%) of 15 in the low- and high-concentration PRP groups, 9 (60%) of 15 in the PPP group, and 8 (53%) of 15 in the control group.

Quantitative analysis of the callus to cortex width ratio and callus area showed that both started to increase from week 2 and reached the peak at week 4. Higher callus to cortex width ratio and callus area of medium-concentration PRP was shown at weeks 2 ($P < .05$) and 4 ($P < .01$) after injection compared with the other groups, suggesting enhanced callus formation. At week 4 after injection, an average 30% increase in callus to cortex width ratio and 50% increase in callus area were found in medium-concentration PRP compared with the control. The callus started to remodel at the late stage of fracture healing. At week 8 after injection, higher callus area was observed in the high-concentration PRP group ($P < .05$), whereas similar callus to cortex width ratio and callus area were observed among the other groups ($P > .05$) (Figures 4B, C).

Three-point Load Bearing

In general, in terms of load to failure value and stiffness, the mechanical properties were higher in the PRP group than in the control and PPP groups. A 50% increase in peak failure load and a 70% in-

crease in stiffness in the medium-concentration PRP group compared with control group were found (Table 3).

Histologic Evaluation

Medium-concentration PRP showed the best performance in accelerating bone healing. Two weeks after injection, newly formed woven bone, inflammatory cells, and vessels were observed adjacent to the fracture site in hematoxylin-eosin stained sections in each group. Four weeks after treatment, the medium-concentration PRP group showed more than 50% trabecular bone formation and cortex remodeling. Bone trabeculae were surrounded by active osteoblasts and resorptive osteoclasts. In comparison, the control and PPP groups mainly demonstrated the appearance of woven (endochondral) bone and cartilage islands spreading throughout the callus. At 8 weeks after injection, well-organized cortex and adult type marrow were observed in 80% of the medium-concentration PRP group. In comparison, immature bone trabeculae were mixed with chondroid tissue in the other groups (Figure 5).

DISCUSSION

Osteoporosis is characterized by increased bone resorption and decreased bone formation. Aged BMSCs derived from osteoporotic bone show an altered epigenetic expression (ie, higher adipogenic tendency and lower osteogenesis capacity). This suppresses osteoblastogenesis and causes a consequent inability to produce a sufficient number of functional osteoblasts for bone formation.¹³ The adipogenesis predominance and osteogenesis inhibition of BMSCs are the main cause of delay in the healing of osteoporotic fractures. In the healing of osteoporotic fractures, a greater amount of pro-osteoclastogenic cytokines, such as receptor activator nuclear factor kappa-B ligand and macrophage colony-stimulating factor, higher amount of osteoblast inhibitors Dickkopf-1 and sclerostin, are produced.¹⁴

Most of the current strategies used in treating osteoporotic fractures involve bone resorption inhibitors. However, these agents cannot promote bone callus formation. Therefore, increasing osteoblastogenetic differentiation and simultaneously suppressing BMSC adipogenesis can promote bone formation, enhancing the healing of osteoporotic fractures.

Platelet-rich plasma contains 30 autologous growth factors reported to enhance osteogenesis.¹⁵ When activated, a 7-fold increase of TGF- β , 30-fold increase of platelet-derived growth factor, and 10-fold increase of vascular endothelial growth factor could be seen in the PRP compared with the whole blood.¹⁶ Platelet-derived growth factor is a key factor that can increase the migration and proliferation of BMSCs.¹⁷ Transforming growth factor- β stimulates the proliferation and differentiation of osteoblasts but inhibits the differentiation of adipocytes.¹⁸ Vascular endothelial growth factor induces endothelial cell proliferation and vascularization.¹⁹ Besides its osteogenesis-promoting ability, PRP is able to decrease the formation of tartrate resistant acid phosphatase-positive multinucleated cells and increase the secretion of osteoprotegerin, thus suppressing osteoclastogenesis and bone resorption.²⁰

Huang and Wang²¹ reported that medium-concentration PRP stimulates BMSC proliferation and osteogenic differentiation. Kawasumi et al²² reported that BMSC proliferation and bone formation were more prevalent in the highest concentration of PRP ($4.3 \times 10^9/\text{mL}$). Arpornmaeklong et al²³ reported that PRP ($3.5 \times 10^9/\text{mL}$) had a dose-dependent stimulation of BMSC proliferation while reducing ALP activity and calcium deposition. In the current study, PRPs were capable of up-regulating the proliferation of aged BMSCs. Medium-concentration PRP ($2.65 \pm 0.2 \times 10^9/\text{mL}$) promotes osteogenic differentiation and also inhibits the adipogenic differentiation of aged BMSCs. However, high-concentration

PRP ($8.21 \pm 0.4 \times 10^9/\text{mL}$) inhibited osteogenic BMSC differentiation. Low-concentration PRP ($0.85 \pm 0.16 \times 10^9/\text{mL}$) and PPP ($8 \pm 0.5 \times 10^6/\text{mL}$) show no capability in the mitogenic and osteoinductive stimulation of BMSCs.

Many in vivo studies have reported that fracture healing in osteoporotic bone appears to be delayed with respect to callus mineralization and biomechanical properties. Osteoporosis seems to delay callus maturation and consequently decelerate fracture healing.¹³ Wang et al²⁴ reported that callus bone mineral density was 18.0% lower in the osteoporosis group 12 weeks after fracture. Callus failure load was 28.8% lower in the osteoporosis group. Endochondral bone formation was delayed, and the new bone trabeculae were arranged loosely and irregularly. Namkung-Matthai et al² reported a 40% reduction in fracture callus cross-sectional area and a 23% reduction in bone mineral density, a 3-fold decrease in peak failure load, and a 2-fold decrease in stiffness in the osteoporotic rats.

The current authors found a 30% increase in callus to cortex width ratio, 50% increase in callus area, 50% increase in peak failure load, and a 70% increase in stiffness in the medium-concentration PRP group compared with the control group. During the fracture healing process, histological evaluation demonstrated an increased appearance of trabecular bone formation and cortex remodeling in the fractures treated with PRP, suggesting acceleration of bone mineralization. In comparison, the control group showed woven bone and cartilage islands spreading throughout the callus at week 8 after injection. Large-volume calluses were observed in the high-concentration PRP group. High-concentration PRP might inhibit the remodeling of trabecular bone in callus by suppressing osteoclastogenesis, and therefore inhibit bone remodeling.²⁰

Limitations of this study include the use of an artificial culture supplemented with PRP, which differs from the environ-

ment in vivo and might not represent the best medium for BMSCs. Finally, quantitative analysis of histomorphology was not performed due to a lack of necessary apparatuses.

CONCLUSION

The in vitro experiments indicated that PRP could simultaneously promote osteoblastogenesis and suppress adipogenesis of aged BMSCs. Medium-concentration PRP ($2.65 \pm 0.2 \times 10^9/\text{mL}$) seemed to be the optimal concentration. High-concentration PRP promoted proliferation but inhibited the osteogenic differentiation of the BMSCs. The in vivo study showed that medium-concentration PRP substantially enhanced osteoporotic fracture repair in the long bones of ovariectomized rats. Further in vivo investigations should be performed to fully reveal the characteristics of the relationship between PRP and osteoporotic fractures. 

REFERENCES

1. Rachner TD, Khosla S, Hofbauer LC. Osteoporosis: now and the future. *Lancet*. 2011; 377(9773):1276-1287.
2. Namkung-Matthai H, Appleyard R, Jansen J, et al. Osteoporosis influences the early period of fracture healing in a rat osteoporotic model. *Bone*. 2001; 28(1):80-86.
3. Abdallah BM, Haack-Sorensen M, Fink T, Kassem M. Inhibition of osteoblast differentiation but not adipocyte differentiation of mesenchymal stem cells by sera obtained from aged females. *Bone*. 2006; 39(1):181-188.
4. Sarban S, Senkoylu A, Isikan UE, Korkusuz P, Korkusuz F. Can rhBMP-2 containing collagen sponges enhance bone repair in ovariectomized rats? A preliminary study. *Clin Orthop Relat Res*. 2009; 467(12):3113-3120.
5. Hollinger JO, Onikepe AO, MacKrell J, et al. Accelerated fracture healing in the geriatric, osteoporotic rat with recombinant human platelet-derived growth factor-BB and an injectable beta-tricalcium phosphate/collagen matrix. *J Orthop Res*. 2008; 26(1):83-90.
6. Chevallier N, Anagnostou F, Zilber S, et al. Osteoblastic differentiation of human mesenchymal stem cells with platelet lysate. *Bio-materials*. 2010; 31(2):270-278.
7. Simman R, Hoffmann A, Bohinc RJ, Peterson WC, Russ AJ. Role of platelet-rich plasma in acceleration of bone fracture healing. *Ann Plast Surg*. 2008; 61(3):337-344.

8. Gandhi A, Dumas C, O'Connor JP, Parsons JR, Lin SS. The effects of local platelet rich plasma delivery on diabetic fracture healing. *Bone*. 2006; 38(4):540-546.
9. Bielecki T, Gazdzik TS, Szczepanski T. Benefit of percutaneous injection of autologous platelet-leukocyte-rich gel in patients with delayed union and nonunion. *Eur Surg Res*. 2008; 40(3):289-296.
10. Jiang Y, Zhao J, Genant HK, Dequeker J, Geusens P. Long-term changes in bone mineral and biomechanical properties of vertebrae and femur in aging, dietary calcium restricted, and/or estrogen-deprived/-replaced rats. *J Bone Miner Res*. 1997; 12(5):820-831.
11. Liu Y, Zhou Y, Feng H, Ma GE, Ni Y. Injectable tissue-engineered bone composed of human adipose-derived stromal cells and platelet-rich plasma. *Biomaterials*. 2008; 29(23):3338-3345.
12. Liu Y, Tan J, Li L, et al. Study on the molecular mechanisms of dlk1 stimulated lung cancer cell proliferation [in Chinese]. *Zhongguo Fei Ai Za Zhi*. 2010; 13(10):923-927.
13. Giannoudis P, Tzioupis C, Almalki T, Buckley R. Fracture healing in osteoporotic fractures: is it really different? A basic science perspective. *Injury*. 2007; (38 suppl 1):90-99.
14. D'Amelio P, Roato I, D'Amico L, et al. Bone and bone marrow pro-osteoclastogenic cytokines are up-regulated in osteoporosis fragility fractures. *Osteoporos Int*. 2010; 22(11):2869-2877.
15. Marx RE, Carlson ER, Eichstaedt RM, et al. Platelet-rich plasma: growth factor enhancement for bone grafts. *Oral Surg Oral Med Oral Pathol Endonotol*. 1998; 85(6):638-646.
16. Babbush CA, Kevy SV, Jacobson MS. An in vitro and in vivo evaluation of autologous platelet concentrate in oral reconstruction. *Implant Dent*. 2003; 12(1):24-34.
17. Gruber R, Karreth F, Kandler B, et al. Platelet-released supernatants increase migration and proliferation, and decrease osteogenic differentiation of bone marrow-derived mesenchymal progenitor cells under in vitro conditions. *Platelets*. 2004; 15(1):29-35.
18. Mehta S, Watson JT. Platelet rich concentrate: basic science and current clinical applications. *J Orthop Trauma*. 2008; 22(6):432-438.
19. Boyapati L, Wang HL. The role of platelet-rich plasma in sinus augmentation: a critical review. *Implant Dent*. 2006; 15(2):160-170.
20. Ogino Y, Ayukawa Y, Kukita T, Atsuta I, Koyano K. Platelet-rich plasma suppresses osteoclastogenesis by promoting the secretion of osteoprotegerin. *J Periodontol Res*. 2009; 44(2):217-224.
21. Huang S, Wang Z. Influence of platelet-rich plasma on proliferation and osteogenic differentiation of skeletal muscle satellite cells: an in vitro study. *Oral Surg Oral Med Oral Pathol Oral Radiol Endod*. 2010; 110(4):453-462.
22. Kawasumi M, Kitoh H, Siwicki KA, Ishiguro N. The effect of the platelet concentration in platelet-rich plasma gel on the regeneration of bone. *J Bone Joint Surg Br*. 2008; 90(7):966-972.
23. Arpornmaeklong P, Kochel M, Depprich R, Kubler NR, Wurzler KK. Influence of platelet-rich plasma (PRP) on osteogenic differentiation of rat bone marrow stromal cells. An in vitro study. *Int J Oral Maxillofac Surg*. 2004; 33(1):60-70.
24. Wang JW, Li W, Xu SW, et al. Osteoporosis influences the middle and late periods of fracture healing in a rat osteoporotic model. *Chin J Traumatol*. 2005; 8(2):111-116.